ACCOUNTS
of chemical research

Gas Transport across Hyperthin Membranes

MINGHUI WANG, VACLAV JANOUT, AND STEVEN L. REGEN*

Department of Chemistry, Lehigh University, Bethlehem, Pennsylvania 18015, United States

RECEIVED ON SEPTEMBER 4, 2012

CONSPECTUS

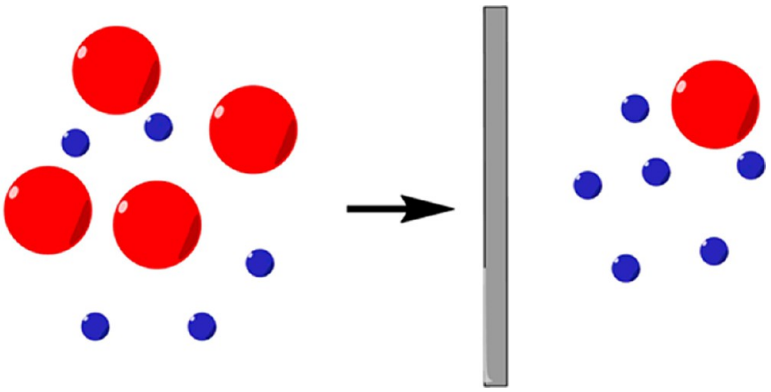

The use of organic polymeric membranes to separate gaseous mixtures provides an attractive alternative to other methods such as selective adsorption and cryogenic distillation. The primary advantages of membrane-based separations are their relative energy efficiency and lower costs. Because the flux of a gas across a membrane is inversely proportional to the membrane's thickness, this method relies on fabricating membranes that are as thin as possible. However, as researchers have tried to produce "hyperthin" membranes (less than 100 nm), these membranes often form defects and lose their permeation selectivity.

In this Account, we review some of the progress in our laboratories at Lehigh University to create hyperthin membranes with high permeation selectivities. We focus special attention on gaseous permeants that are relevant for the production of clean energy (H_2 and CO_2 formed from CH_4) and the reduction of global warming (CO_2 and N_2, the major components of flue gas). Our studies make extensive use of Langmuir–Blodgett (LB) methods and porous surfactants derived from calix[6]arenes. We specially designed each surfactant to form cohesive monolayers and multilayers, and we introduced a "gluing" technique, where we cross-link porous surfactants containing quaternary ammonium groups ionically with polymeric counterions. Using ellipsometry, atomic force microscopy, X-ray photoelectron spectroscopy, monolayer isotherm, surface viscosity, and permeation measurements, we have characterized these hyperthin films. While molecular sieving appears to make a significant contribution to the permeation selectivity of some of these membranes, solution-diffusion pathways predominate. We also describe initial studies in which we formed hyperthin films from poly(ethylene glycol)-based polyelectrolytes using layer-by-layer deposition (LbL) methods. We have found remarkably high H_2/CO_2 and CO_2/N_2 permeation selectivities with these LB- and LbL-based hyperthin membranes. These results suggest that such materials may lead the way to materials that researchers can exploit to purify hydrogen produced from CH_4 and to capture CO_2 from flue gas.

1. Introduction

The ability to separate gaseous mixtures efficiently and economically has important practical implications; for example, the production of clean energy and the reduction of global warming.[1−4] Although adsorption and cryogenic distillation are commonly used for this purpose, both of these methods are costly in terms of their energy and capital requirements.[5,6] For this reason, attention has begun to focus on membrane technology as an alternative.[7−11] Some polymeric membranes are, in fact, already in use for separating the following mixtures: O_2/N_2, H_2/N_2, H_2/CH_4, and H_2/CO.[7] At present, viable membranes are being sought for H_2/CO_2 (for the purification of hydrogen produced from CH_4) and for CO_2/N_2 (for the capturing of CO_2 from flue gas).[7]

Two key properties of membranes that define their practical potential are the *flux* that can be produced across

Published on the Web 01/29/2013 www.pubs.acs.org/accounts
10.1021/ar3002624

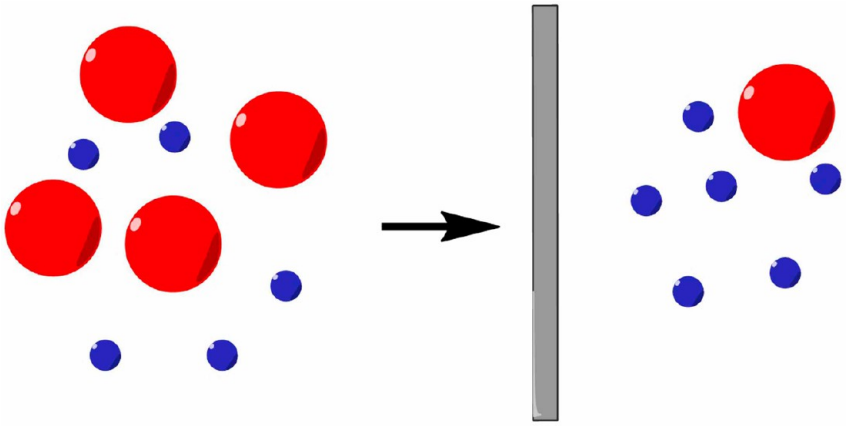

FIGURE 1. Gaseous permeants, *i* (small gaseous permeant, blue) and *j* (large gaseous permeant, red) diffusing across a polymeric membrane.

them and their *permeation selectivity*. From a basic science standpoint, learning how to create membranes that allow for a high flux and high selectivity is the primary goal. From a technological standpoint, maximizing the surface area and mechanical and thermal stability of a membrane while minimizing its cost of production are the main issues. Before discussing our own basic science efforts in this area, we briefly review the solution-diffusion model, which is commonly used to characterize gas transport across polymeric membranes.[7]

Figure 1 shows a stylized illustration of two hypothetical gas molecules (*i* and *j*) diffusing across a polymeric membrane. According to the solution-diffusion model, the flux (J) of each gas is related to its permeability coefficient (P), the pressure gradient (Δp) that is applied across the membrane, and the thickness of the membrane (l) as shown in eq 1. Rearrangement to eq 2 expresses this relationship in terms of a normalized flux or "permeance", P/l. The membrane's permeation selectivity, α, is then defined by the ratio of the two permeances (eq 3). Since the permeability coefficient is also equal to the product of diffusivity (D) and solubility (S) coefficients, the permeation selectivity may also be expressed as shown in eq 4.

$$J(\mathrm{cm}^3/[\mathrm{cm}^2\cdot\mathrm{s}]) = \frac{P\Delta p}{l} \tag{1}$$

$$\frac{P}{l}(\mathrm{cm}^3/[\mathrm{cm}^2\cdot\mathrm{s}\cdot\mathrm{cmHg}]) = \frac{J}{\Delta p} \tag{2}$$

$$\alpha_{ij} = \frac{\left(\frac{P}{l}\right)_i}{\left(\frac{P}{l}\right)_j} \tag{3}$$

$$\alpha_{ij} = \left(\frac{D_i}{D_j}\right)\left(\frac{S_i}{S_j}\right) \tag{4}$$

Permeability coefficients are often dominated by a permeant's diffusivity across or solubility within a given membrane. In some cases, both factors have similar weight, a situation that can make membrane-based separations especially challenging. A prime example of this is the separation of H_2 from CO_2. Here, the relatively low diffusivity of the larger CO_2 molecule is counterbalanced by its greater solubility in polymeric membranes; the net result is that both permeants have similar permeability coefficients.[7]

In this Account, we review some of the progress that has been made in our laboratories at Lehigh University in creating *hyperthin membranes* (i.e., membranes that are less than 100 nm in thickness) having *high permeation selectivities*. Because of the inverse relationship between flux and membrane thickness, it is desirable to fabricate membranes as thin as possible (eq 1). In general, as thickness goes below ca. 100 nm, it has proven difficult to avoid defects from being formed and, as a consequence, reduced selectivity is commonly observed.[12,13] In principle, the creation of hyperthin membranes that are free of defects should offer fundamentally new opportunities for gas separations.

2. Conventional Langmuir–Blodgett Films

2.1. An Early Vision. In early pioneering studies, Katherine Blodgett proposed that Langmuir–Blodgett (LB) films might be employed as "sieves or filters for the segregation of previously `non-filterable' substances of molecular magnitudes. It is only necessary for such filtration that the particles or molecules to be filtered be of a size greater than the dimensions of the molecular voids formed in the film structure."[14] This hypothesis has encouraged many researchers to investigate LB films as novel membrane materials.

While more sophisticated methods for fabricating LB films have evolved in recent years (e.g., Figure 2), the essential

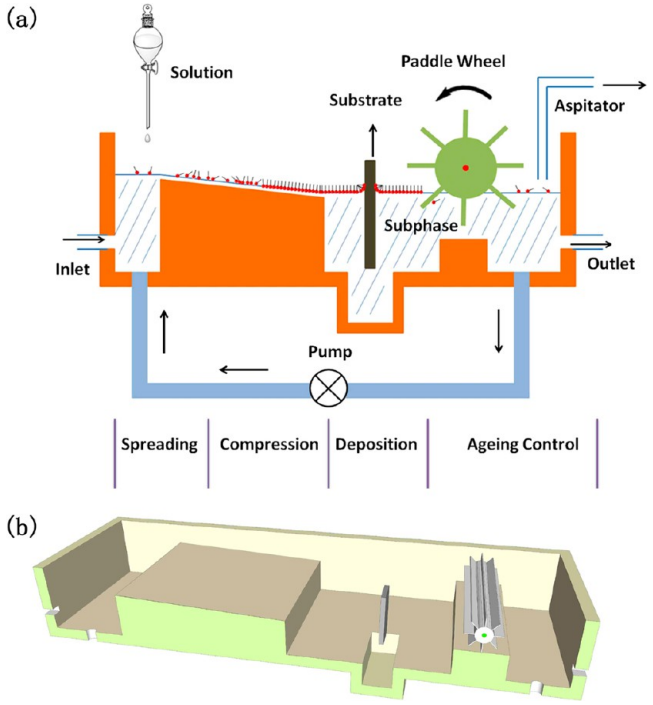

FIGURE 2. Side view of a continuous LB film deposition apparatus shown in (a) two and (b) three dimensions.[15]

features of Blodgett's approach have remained unchanged; that is, one first forms a surfactant monolayer at the air/water interface and then transfers it to a solid support by passing the support vertically through the monolayer.[15] Most commonly, LB films are of the Y-type in which the monolayers are in a head-to-head and tail-to-tail arrangement.

2.2. Langmuir–Blodgett Membranes for Gas Separations. Despite many attempts to use LB films for gas separations, most studies have proven disappointing. In nearly all instances, permeation selectivities have been less than what is predicted from Graham's law, a finding that indicates that gas transport occurs mainly through defects. For example, LB multilayers of stearic acid, deposited onto a silicone copolymer, exhibited He/N_2 selectivities that were less than the Graham's law value of 2.6, even when 48 monolayers that were 120 nm in thickness were used.[16,17]

In one rare example of permeation selectivity exceeding Graham's law, a LB film that was constructed from 40 monolayers (58 nm) of a polymeric surfactant ($X = 90\%$ and $Y = 10\%$) exhibited a He/N_2 selectivity of ca. 23 (Figure 3).[18]

3. Perforated LB Bilayers

3.1. Design Strategy. To improve upon the gas permeation selectivity of LB films, we sought to create *perforated monolayers from porous surfactants*. Our working hypothesis

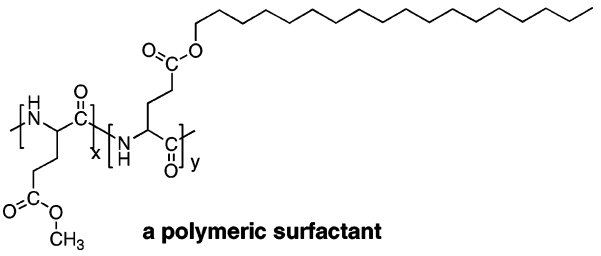

FIGURE 3. Structure of a polymeric surfactant used in forming a LB film.

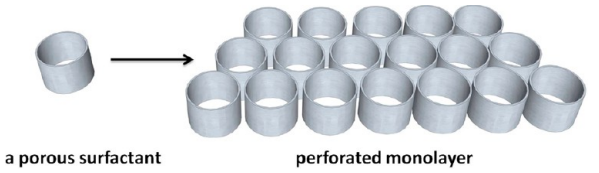

FIGURE 4. A stylized illustration of a perforated monolayer derived from a porous surfactant.

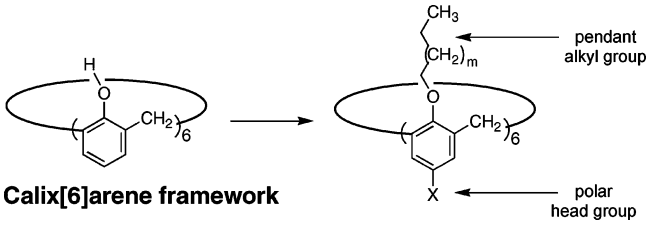

FIGURE 5. A porous surfactant derived from a calix[6]arene framework.

has been that such membranes would act like molecular sieves and that the presence of multiple hydrocarbon chains within each surfactant would enhance the cohesiveness of these assemblies, thereby minimizing defect formation (Figure 4). On the basis of this idea, we have made extensive use of the calix[6]arene framework in synthesizing a variety of porous surfactants (Figure 5).[19–22] Examination by space filling models indicate that this framework has a *maximum* internal pore diameter of 0.48 nm. Because of the conformational freedom of the calix[6]arene framework and also because of the potential for pendant alkyl chains to "fold" into the pore, the effective diameter of such surfactants is expected to be somewhat less than this value.[19]

Three generations of calix[6]arene-based surfactants that we have designed as part of this program are shown in Figure 6. A first generation contains disulfide moieties that are available for photo-cross-linking.[23,24] A second generation has amide oxime head groups that can produce a cohesive assembly via hydrogen bonding with nearest neighbors.[25,26] A third generation bears quaternary ammonium-based groups, which can yield ionically cross-linked

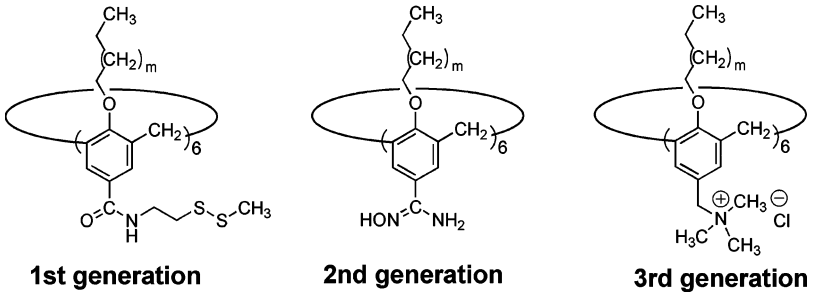

FIGURE 6. Three generations of calix[6]arene-based surfactants.

SCHEME 1. Synthetic Scheme Used To Prepare **1**

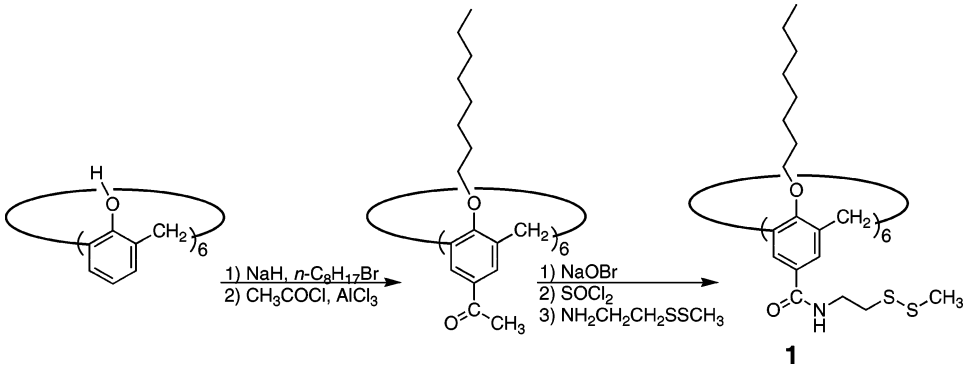

(i.e., "glued together") monolayers with polymeric counterions that are picked up from the aqueous subphase.[27]

3.2. First Generation Calix[6]arene-Based Surfactants. The synthetic method that we used to prepare a first-generation surfactant, **1**, is outlined in Scheme 1.[23,24] As expected, **1** showed well-behaved monolayer properties at the air/water interface, with a collapse pressure of 53 mN/m and an occupied area of 1.65 nm^2/molecule at this pressure.[24] This occupied area is fully consistent with an orientation in which all of the amide groups are in contact with the water surface and the alkyl chains extend into air. As expected, brief exposure to UV light (254 nm) resulted in cross-linking, as evidenced by surface viscosity measurements.[24]

Multilayers of **1** that were deposited onto Celgard (a stretched form of polypropylene having pores that were ca. 400 × 40 nm) and Nuclepore membranes (having cylindrical pores of ca. 30 nm diameter that extend from one face of the membrane to the other) resulted in a reduction in He and N_2 flux across such supports, but He/N_2 selectivities that were less than 2.6. In contrast, deposition of a *single* bilayer of **1** onto poly[1-(trimethylsilyl)-1-propyne] (PTMSP), a glassy polymer having a contiguous network of ca. 1 nm pores, gave a He/N_2 selectivity of ca. 7. Deposition of a second bilayer of **1** led to only a slight increase in selectivity. Exposure to UV light then resulted in polymerization of the assembly but did not improve the permeation selectivity. Instead, this UV treatment resulted in the photodecomposition of the support.[24]

3.3. Second Generation Calix[6]arene-Based Surfactants. Second generation calix[6]arene-based surfactants were synthesized as shown in Scheme 2.[25,26] Caxli[6]arenes **2a** and **2b** exhibited well-behaved monolayer properties with collapse pressures in excess of 60 mN/m. Significantly, **2a** and **2b** showed *the same limiting area* of ca. 1.70 nm^2/molecule. This fact, in and of itself, provides compelling evidence that both surfactants are oriented in the same way at the air/water interface; that is, with their hydrocarbon tails extending into air and their amide oxime groups in contact with the water surface.

When two bilayers of **2a** or **2b** were deposited onto PTMSP, we observed He/N_2 permeation selectivities of ca. 20. In sharp contrast, when two bilayers of conventional single-chain surfactants (i.e., arachidic acid or stearoylamide oxime) were deposited onto PTMSP, no permeation selectivity was observed. Further investigation by FTIR and X-ray photoelectron spectroscopy (XPS) provided evidence that bilayers made from the single-chain surfactant stearoylamide oxime underwent *disassembly* on the surface of PTMSP

SCHEME 2. Synthesis of Second Generation Calix[6]arene-Based Surfactants

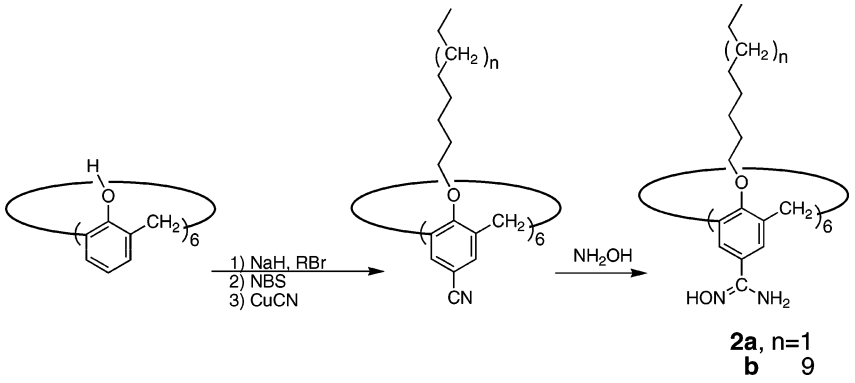

SCHEME 3. Synthesis of a Third Generation Calix[6]arene-Based Surfactant

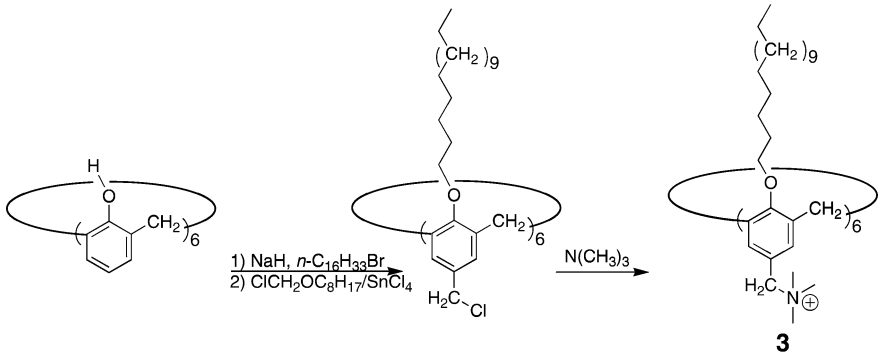

and *absorption* into the bulk polymer phase. Analogous measurements further showed that the calix[6]arene-based surfactant was fully retained on the PTMSP surface. We posited that the stability of the calix[6]arene-based LB film on the PTMSP surface was a likely consequence of its larger size (outer diameter is ca. 1.4 nm), which can span ca. 1.0 nm pores of the glassy PTMSP film, thereby preventing disassembly and absorption.

3.4. Third Generation Calix[6]-arene-Based Surfactants. In Scheme 3, we show the synthetic methods that we used to prepare a third generation calix[6]arene-based surfactant, **3**.

3.4.1. Gluing with Poly(4-styrenesulfonate) (PSS). When spread over a pure aqueous subphase, monolayers of **3** were found to be more compressible than ones formed from **1**, **2a**, and **2b**; that is, the "lift-off" and collapse points extend over a larger range of areas per molecule.[27,28] At its collapse pressure (ca. 40 mN/m), **3** occupied an area of ca. 1.85 nm^2. When spread over an aqueous subphase containing poly(4-styrenesulfonate) (PSS), similar isotherms were observed. Evidence for ionic cross-linking of **3** by PSS in the monolayer state was then obtained via surface viscosity measurements; that is, the presence of PSS in the aqueous subphase significantly increased the monolayer's surface viscosity.[28] Evidence for incorporation of PSS into single LB bilayers of **3** was then obtained by a combination of ellipsometry and XPS measurements. Thus, in the absence of PSS, the thickness of a bilayer of **3** was 4.80 nm. A similar bilayer that was prepared in the presence of PSS showed a film thickness of 5.64 nm. Further analysis by XPS for nitrogen (N) and sulfur (S), using various "take-off" angles, showed that both elements were buried within the LB bilayer. Moreover, the fact that the N/S atomic ratio of 0.38 $\pm$ 0.09 showed a negligible dependency on the takeoff angle used further indicated that both atoms lie at a similar depth within the bilayer. Based on atomic percentages for Na, N, S, and Cl, we were able to conclude that ion exchange was essentially complete and that the glued bilayer contains a ca. 2-fold excess of sodium 4-styrene sulfonate groups. Enhanced stability via gluing was readily apparent by the fact that the glued bilayer of **3** (unlike the unglued analog) was stable toward chloroform. A stylized illustration of a PSS-glued bilayer of **3** is shown in Figure 7.

Examination of glued versus unglued LB bilayers of **3** further revealed that gluing significantly enhances the

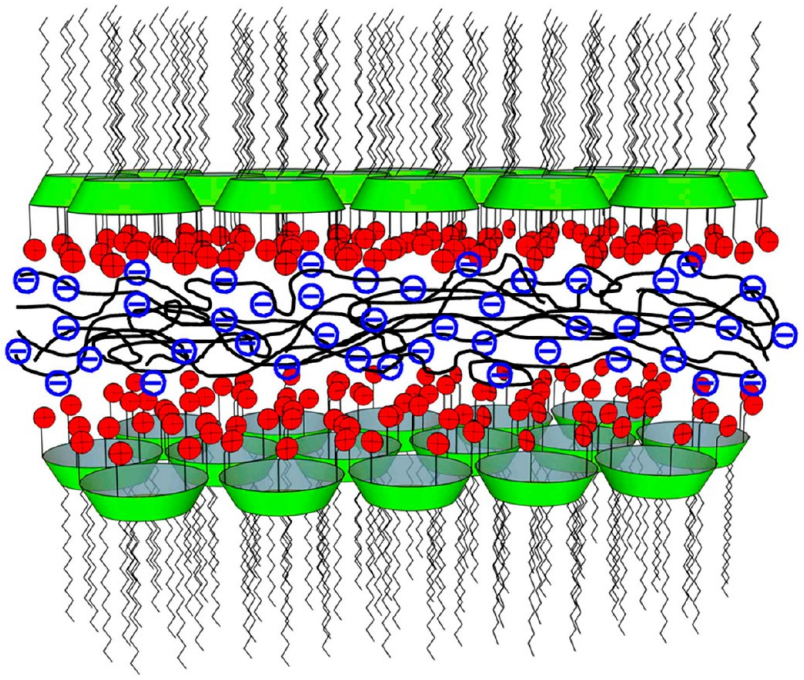

FIGURE 7. Stylized illustration of a LB bilayer of **3** that has been glued together with PSS.

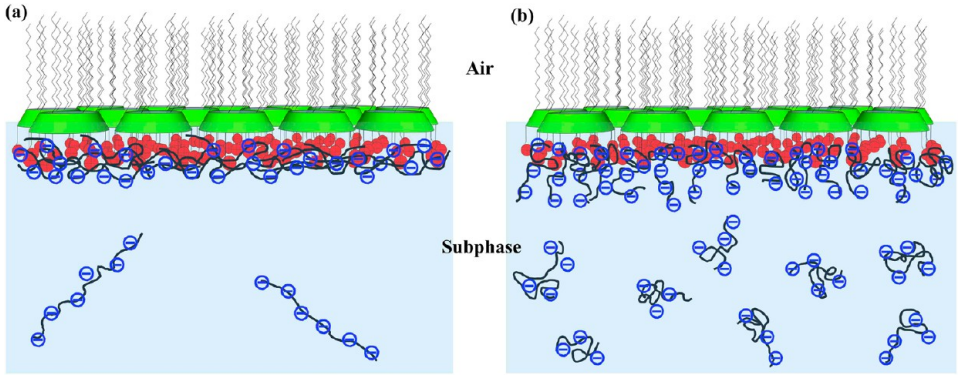

FIGURE 8. Stylized illustration showing (a) a monolayer that is highly cross-linked by polymeric counterions with relative few polymer chains in solution and (b) a monolayer that has a relatively low cross-link density and a large number of polymer chains in solution. Note, the polymer chains in the subphase in (panel b) are shown in a more coiled state due to a higher ionic strength that reduces the repulsion of neighboring charge along the polymer backbone.

barrier properties and permeation selectivity of such assemblies.[28] Thus, whereas an unglued bilayer of **3** exhibited a modest He/N_2 selectivity of ca. 30, a corresponding glued bilayer showed a He/N_2 selectivity of ca. 170.

In related studies, the gluing of **3** was found to be strongly dependent on the concentration of PSS that was present in the subphase. Thus, as the repeat unit concentration decreased from 5.0 to 1.0 and to 0.1 mM, the surface viscosity of monolayer of **3** steadily increased, reflecting a higher degree of ionic cross-linking.[29] Although LB transfer was effective with moderate surface viscosities using a 5.0 mM repeat unit concentration, higher viscosities made LB transfer difficult, as judged by transfer ratios, that is, the decrease in monolayer area at the air/water interface divided by the geometrical surface area of the substrate passing through the interface. Additionally, when glued LB bilayers were fabricated using a repeat unit concentration that was less than 5.0 mM, their He/N_2 permeation selectivities were reduced, reflecting the likely presence of defects.

This strong dependency of gluing on the concentration of PSS can be accounted for by a competition for ion exchange between free sulfonate groups of PSS polymers that have become bound to the surfactant monolayer with sulfonate groups of PSS that are in the bulk aqueous phase. Thus,

when a low PSS concentration is used, the effective concentration of monolayer-bound PSS becomes relatively high, making it more effective in undergoing ion exchange with the remaining quaternary ammonium groups; the net result is a higher degree of ionic cross-linking (Figure 8). This explanation leads to the prediction that the amount of PSS that is taken up in a glued bilayer should decrease with decreasing concentrations of PSS in the subphase, and this has been confirmed by XPS analysis.[29]

3.4.2. Gluing with Poly(acrylic acid) (PAA). The use of a weak polyacid to cross-link monolayers of **3** was also of interest to us since pH should allow one to fine-tune its gluing strength. In principle, by lowering the pH (the pK_a of PAA is ca. 4.5), one might expect that increased hydrophobicity due to protonation of the carboxylic groups would contribute to gluing via hydrophobic interactions plus hydrogen bonding, while reducing the extent of ionic association. It is noteworthy, in this regard, that a previous study has shown that the ability of PAA to form "complexes" with phospholipid monolayers and bilayers increases as the pH is lowered below 4.0.[30]

In exploring PAA as a gluing agent, we first examined the pH dependency of monolayers of **3** over an aqueous subphase containing 0.1 mM PAA.[31] At pH of 10.0, the isotherm behavior and the surface viscosity of these monolayers were similar to that found in the absence of PAA. However, upon lowering the pH to 4.4, the area that was occupied by **3** increased, suggesting that there was partial penetration of the polymer into the surfactant monolayer. Also, the surface viscosity of the monolayer was found to increase as the pH was lowered.

Single LB bilayers of **3** that were deposited onto PTMSP in the presence of 0.1 mM PAA showed a significant dependence of the uptake of the polymer on pH. Thus, examination of two such surfaces by XPS (one prepared at pH 10 and one fabricated at pH 4.4) showed considerably more polymer being taken up at the lower pH.[31] This was evident by comparing the atomic compositions for the carboxyl carbon and the quaternary ammonium nitrogen. Thus, the molar ratio of carboxylate to quaternary ammonium groups was estimated to be 3.3 for bilayers prepared at pH 4.4. When a pH of 10.0 was used for Langmuir–Blodgett deposition, this ratio was reduced to ca. 0.4. Analysis by ellipsometry confirmed that the uptake of PAA was greater at a lower pH. Thus, the thicknesses of bilayers that were glued with PAA at pH 4.4 and 10.0 were 5.4 and 4.9 nm, respectively. In the absence of PAA, the thickness of bilayers of **3** was 4.6 nm.

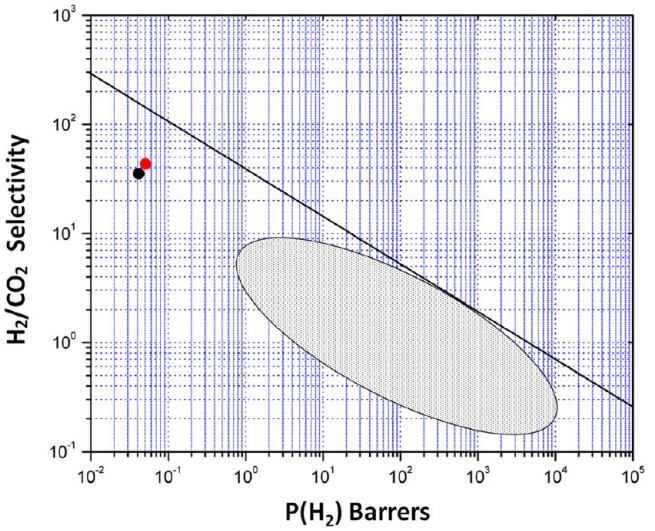

FIGURE 9. Upper bound plot for H_2/CO_2 selectivity versus H_2 permeability, P_{H_2}. Here, the shaded oval represents the region that covers most of the polymers that have been reported to date. Also shown are the intrinsic barrier properties of PAA-glued bilayers of **3** (●), which have been calculated using the series resistance model.

Given the strong pH dependence on gluing, we expected to observe a strong pH dependence on the membrane's barrier properties. In fact, the He/N_2 selectivity of PAA-glued bilayers of **3** reached 1000 when a pH of 4.4 was used; with a pH of 10, this selectivity was reduced to 110. The high selectivity at low pH strongly encouraged us to investigate the barrier properties of such membranes toward H_2 and CO_2.[32] To our delight, we found that a bilayer of **3** that was glued with PAA at pH 3.3 exhibited H_2/CO_2 permeation selectivities that ranged from 35 to 70. Given the hyperthin nature of these separating layers (ca. 6 nm in thickness), this level of permeation selectivity is extraordinary.

To place the barrier properties of these hyperthin membranes into perspective, we have calculated their intrinsic permeability using the series-resistance model and have included them in an "upper-bound" plot for H_2/CO_2.[16,17,33] Thus, if it is assumed that the resistance of the composite (i.e., the reciprocal of its permeance) is equal to the resistance of the LB bilayer plus that of the PTMSP, then the permeance of the bilayer, $[P/l]_{LB}$, can be calculated from the equation, $1/[P/l]_{composite} = 1/[P/l]_{PTMSP} + 1/[P/l]_{LB}$. Obviously, as the resistance of the permeation-selective layer approaches that of the support, the latter will make increasingly larger contributions to the overall resistance of the membrane. In this regard, it should be noted that for all the hyperthin/PTMSP composite membranes that we have prepared, the resistance of the hyperthin separating layer was at least 10 times higher than that of the support.

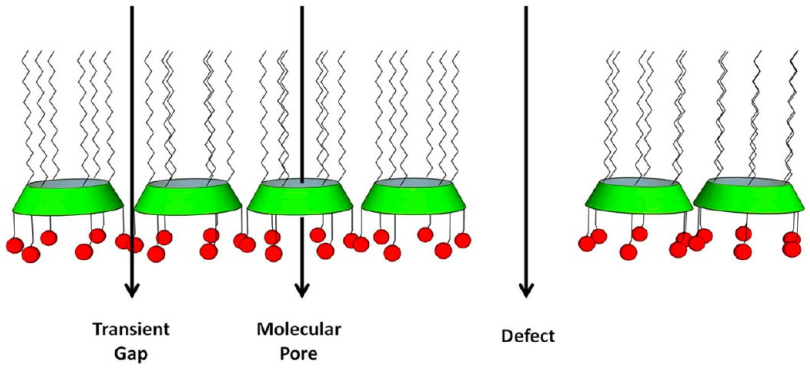

FIGURE 10. A stylized illustration showing possible pathways for transport across a perforated monolayer.

Based on a bilayer thicknesses of 6 nm, one can then calculate its permeability coefficient using the equation: $P_{LB} = [P/l]_{LB}l_{LB}$. Values that have been calculated in this manner have been included in an "upper bound" plot, in which H_2/CO_2 selectivity is plotted as a function of H_2 permeability (Figure 9).[16,17,33] Here, the shaded oval that appears in this figure represents data for a large number of polymeric membranes that have previously been reported.[33] The solid line that is drawn is considered to be the combination of the highest permeability and the highest permeation selectivity that is possible. The fact that these data fall beneath the upper bound implies that the solution-diffusion mechanism is the dominant pathway for permeation. If molecular sieving were dominant, one might expect permeation properties that lie above the upper bound.[34] Finally, we wish to emphasize that although a few homopolymer-based membranes have been reported to have similar H_2/CO_2 permeation selectivities and permeabilities as PAA-glued bilayers of **3**, it is only that latter that can be formed as defect-free, *hyperthin* separating layers in composite membranes, a feature that highlights their attractiveness.

A simple model that can account for the high permeation selectivity found with PAA-glued bilayers of **3** is based on ionic cross-linking plus self-healing. Thus, at low pH, only portions of PAA are ionized and available for ionic cross-linking. The remaining carboxylate groups are protonated and relatively hydrophobic segments. In principle, the latter should be capable of "filling in gaps" by interacting with exposed hydrocarbon regions of the bilayer via hydrophobic interactions, that is, acting like "caulking" material.

4. Evidence for Contributions from Molecular Sieving

If one considers that the maximum internal diameter of the calix[6]arene framework is 0.48 nm and based on the kinetic diameters for He, H_2, CO_2, and N_2, which are 0.26, 0.28, 0.33, and 0.36 nm, respectively, then all of these gases have the potential for crossing calix[6]arene-based LB bilayers by three pathways: (i) diffusion through the individual surfactants, (ii) diffusion through transient gaps that develop between the surfactants as a result of thermal motion, and (iii) diffusion through defects in the film (Figure 10).

Unusual pressure effects that we have observed for the permeance of helium, but not for nitrogen, across a membrane made from three LB bilayers of **2a** lend support for contributions from *diffusion through individual surfactants*.[35] According to the solution-diffusion model, as the pressure gradient of a permeant gas increases, a proportional increase in its flux should be observed (eq 1). In other words, the permeance of a membrane, P/l, is expected to be independent of the pressure gradient (eq 2). Any change in the permeance should, therefore, represent a change in the structure of the membrane. Experimentally, we have found that the permeance for nitrogen across LB bilayers of **2a** is constant over a pressure gradient that ranges from 5 to 25 psi but that the permeance for helium increases with increasing pressures (Figure 11). Additionally, these changes in the permeance for helium were found to be completely reversible.

A model that can account for this difference between He and N_2 is one in which (i) He but not N_2 can diffuse through the individual surfactants and (ii) the degree of alignment of **2a** between the monolayers increases as the helium pressure increases (Figure 12). Thus, this model assumes that there is lateral diffusion of the calix[6]arenes within each monolayer and that a flow of He through a contiguous channel enhances the stability of such a channel.

For analogous glued LB bilayers, the possibility exists that the main barrier for gas transport may be the glue, itself and that the LB bilayer merely acts as a template for "picking

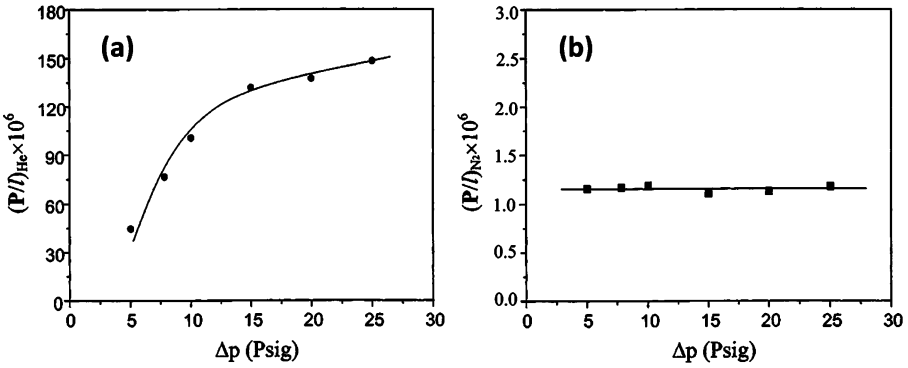

FIGURE 11. The permeance of (a) He and (b) N_2 across an asymmetric membrane formed from PTMSP and six monolayers of **2a** as a function of the applied pressure gradient. All permeance values are in units of $cm^3/[cm^2 \cdot s \cdot cm\ Hg]$.

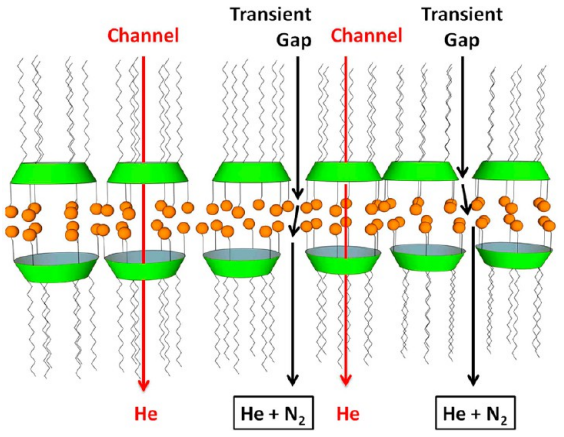

FIGURE 12. A stylized illustration showing a He-induced formation of a contiguous calix[6]arene-based channel in a LB bilayer and nitrogen crossing, exclusively, through transient gaps and defects.

up" a hyperthin form of the polymer. However, experiments that have been carried out using PSS as the glue in the presence of varying concentration of NaCl have provided strong support that it is the combination of the polymer and the surfactant bilayer that serves as the main barrier for gas transport.[36]

5. Layer-by-Layer Hyperthin Films

5.1. Design Strategy. One new avenue that we have begun to explore in this area is the fabrication of hyperthin membranes using layer-by-layer (LbL) deposition methods.[37−42] Prior to our work, the potential of LbL thin films as permeation-selective membranes was established, based on their barrier properties with respect to H_2, N_2, and O_2.[41] In preliminary studies, we demonstrated the feasibility of using PTMSP as a support for LbL multilayers derived from PSS and poly(allylamine hydrochloride) (PAH).[43] Here, a PSS-glued LB monolayer was used to anchor the LbL assembly on the support.[44]

Because CO_2 has a much higher solubility in poly(ethylene glycol)s than H_2, there has been growing interest in synthesizing cross-linked polymers containing poly(ethylene glycol) (PEG) segments for H_2/CO_2 separations.[45,46] Specifically, the goal has been to exploit permeation selectivity that is dominated by solubility differences. In principle, the creation of hyperthin PEG-based membranes that allow for a high flux and high CO_2/H_2 selectivities could lead the way to advanced materials and processes for the purification of hydrogen. With this idea in mind, we have begun to synthesize PEG-based polyanions and polycations using an ion linker strategy (Scheme 4).

5.2. Initial Studies. In initial studies, polymer **4** was synthesized by the sequence of reactions shown in Scheme 5.[47] Using standard layer-by-layer deposition methods, **4** was then combined with PAH to form multilayer assemblies on PTMSP. Hyper-thin membranes containing seven layers of PAH-**4** gave a film thickness of 7 nm. Although the selectivity of this asymmetric membrane toward He/N_2 was substantial (the He/N_2 permeance ratio was 240), its selectivity with respect to He/CO_2 was barely detectable, that is, 0.83. In this case, He was used as a nonflammable surrogate for H_2. However, what proved to be more interesting was the observation of a CO_2/N_2 permeation selectivity that was >280.

In Figure 13, we show an upper bound plot for CO_2/N_2 that has been constructed from data taken from the literature for a variety of polymer membranes, along with the barrier properties of the asymmetric membrane made from PTSMP and a LbL hyperthin film made from **4** and PAH. As is evident, our asymmetric membrane has exceptional selectivity. At present, we believe that an enhanced solubility of CO_2 in this poly(ethylene glycol)-containing assembly, together with a slower diffusivity of the larger N_2 molecule, leads to such selectivity.

SCHEME 4. Ionic Linker Strategy for Creating PEG-Based Polyanions and Polycations

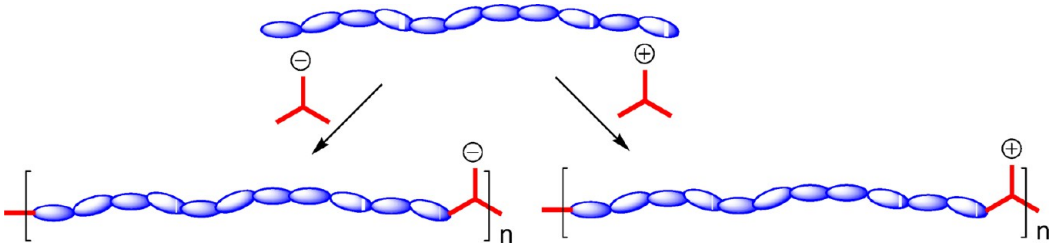

SCHEME 5. Synthesis of a PEG-Based Polyanion and Its Use in Forming LbL Thin Films

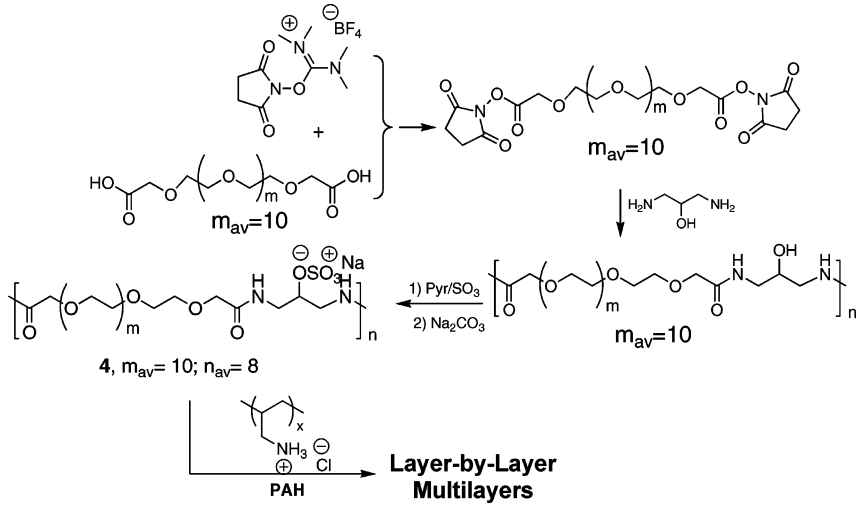

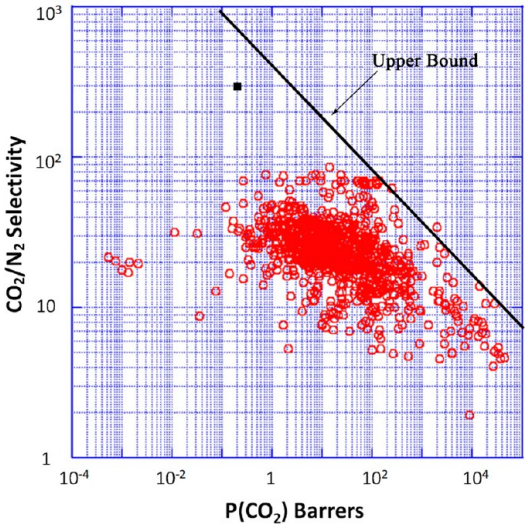

FIGURE 13. Upper bound plot for CO_2/N_2. The red circles show the CO_2/N_2 permeation characteristics (i.e., selectivity and permeability) for a variety of organic polymer membranes that have been reported in the literature (Figure adapted by authors from ref 33). The solid square represents the intrinsic permeation characteristics of the LbL membrane of **4** plus PAH (7 nm in thickness), which have been calculated using the series resistance model.

Hyperthin membranes of this type are now under intensive investigation.

6. Conclusions and Prospects

In this Account, we have shown how hyperthin membranes (<100 nm in thickness) can be fabricated from calix[6]arene-based surfactants using LB methods and PTMSP support material, which have gas permeation selectivities that exceed values predicted from Graham's law. We have also discussed how enhanced cohesiveness of some of these assemblies is possible through electrostatic attraction, hydrophobic interactions, and hydrogen bonding. Although the dominant pathway for permeation across "perforated" LB bilayers appears to involve a solution-diffusion mechanism, evidence has been obtained for contributions from molecular sieving in one such membrane. Recent studies involving hyperthin membranes constructed from poly(ethylene glycol)-containing polyelectrolytes using the LbL method have also shown that such materials have promise for gas separations, especially for the separation of CO_2 from N_2. The relatively high H_2/CO_2 and CO_2/N_2

permeation selectivites that have been found to date offer encouragement that such materials may lead the way to exploitable materials for the purification of hydrogen produced from CH_4, and for the capturing of CO_2 from flue gas. With this thought in mind, studies that are currently in progress are being aimed at modifying the surface of PTMSP-coated hollow fibers and using them as supports for those hyperthin membranes that exhibit the highest H_2/CO_2 and CO_2/N_2 permeation selectivities. In principle, the high surface areas associated with hollow fibers should move this hyperthin membrane approach one step closer to practicality.

The authors are grateful to the U.S. DOE, Office of Basic Energy Sciences, for support of this research under Contract DE-FG02-05ER15720.

BIOGRAPHICAL INFORMATION

Minghui Wang was born in Fenghua, China. He received his B.S. in chemistry from East China Normal University (Shanghai) in 2005 and an M.S. in materials chemistry at Shanghai Institute of Ceramics in 2008. He is currently a Ph.D. student in Polymer Science at Lehigh working under the supervision of S. L. Regen.

Vaclav Janout was born in Prague (Czech Republic). He received his B.S. in chemistry from Charles University (Prague) in 1974 and a Ph.D. in 1978 from the Institute of Macromolecular Chemistry (Prague). He was a Principal Investigator at the Institute of Macromolecular Chemistry from 1982 to 1988 and is currently a Senior Research Scientist at Lehigh University.

Steven L. Regen was born in Brooklyn, NY. He received a B.S. degree in chemistry from Rutgers University in 1968 and Ph.D. from MIT in (1972). He began his independent career in 1972 at Marquette University and moved to Lehigh University in 1985, where he is currently a University Distinguished Professor. His research interests encompass lipids and membrane chemistry, drug delivery, polymer science, and materials chemistry.

FOOTNOTES

The authors declare no competing financial interest.

REFERENCES

1 Marban, G.; Valdes-Solis, T. Towards the hydrogen economy? *Int. J. Hydrogen Energy* **2007**, *32*, 1625–1637.

2 Shao, L.; Low, B. T.; Chung, T.-S.; Greenberg, A. R. Polymeric membranes for the hydrogen economy: Contemporary approaches and prospects for the future. *J. Membr. Sci.* **2009**, *327*, 18–31.

3 Scholes, C. A.; Kentish, S. E.; Stevens, G. W. Carbon dioxide separation through polymeric membrane systems for flue gas applications. *Recent Pat. Chem. Eng.* **2008**, *1*, 52–66.

4 Powell, C. E.; Qiao, G. G. Polymeric CO_2/N_2 gas separation membranes for the capture of carbon dioxide from power plant flue gases. *J. Membr. Sci.* **2006**, *279*, 1–49.

5 Hinchliffe, A. B.; Porter, K. E. A comparison of membrane separation and distillation. *Chem. Eng. Res. Des.* **2000**, *78*, 255–268.

6 Sircar, S.; Golden, T. C. Purification of hydrogen by pressure swing adsorption. *Sep. Sci. Technol.* **2000**, *35*, 667–687.

7 Yampolskii, Y. Polymeric gas separation membranes. *Macromolecules* **2012**, *45*, 3298–3311.

8 Ockwig, N. W.; Nenoff, T. M. Membranes for hydrogen separation. *Chem. Rev.* **2007**, *107*, 4078–4110.

9 Koros, W. J. Membranes: Learning a lesson from nature. *Chem. Eng. Prog.* **1995**, *91*, 68–81.

10 Stern, S. A. Polymers for gas separations: The next decade. *J. Membr. Sci.* **1994**, *94*, 1–65.

11 *Polymers for Gas Separations*; Toshima, N., Ed.; VCH Publishers, Inc.: New York, 1992.

12 Ismail, A. F.; Yean, L. P. Review on the development of defect-free and ultrathin-skinned asymmetric membranes for gas separation through manipulation of phase inversion and rheological factors. *J. Appl. Polym. Sci.* **2003**, *88*, 442–451.

13 Hachisuka, H.; Ohara, T.; Ikeda, K. New type of asymmetric membranes having almost defect-free hyper-thin skin layer and sponge-like porous matrix. *J. Membr. Sci.* **1996**, *116*, 265–272.

14 Blodgett, K. B. Film structure and method of preparation. U.S. Patent, 2,220,860, 1940.

15 Albrecht, O.; Eguchi, K.; Matsuda, H.; Nakagiri, T. Construction and use of LB deposition machines for pilot production. *Thin Solid Films* **1996**, *284−285*, 152–156.

16 Rose, G. D.; Quinn, J. A. Gas transport through supported Langmuir-Blodgett multilayers. *J. Colloid Interface Sci.* **1968**, *27*, 193–207.

17 Rose, G. D.; Quinn, J. A. Composite membranes: The permeation of gases through deposited monolayers. *Science* **1968**, *159*, 636–637.

18 Riedl, T.; Nitsch, W.; Michel, T. Gas permeability of Langmuir-Blodgett (LB) films: Characterization and application. *Thin Solid Films* **2000**, *379*, 240–252.

19 Gutsche, C. D. *Calixarenes*; Royal Society of Chemistry: Cambridge, U.K., 1989.

20 McCullough, D. H., III; Regen, S. L. Don't forget Langmuir-Blodgett films. *Chem. Commun.* **2004**, *24*, 2787–2791.

21 Markowitz, M. A.; Bielski, R.; Regen, S. L. Perforated monolayers: Porous and cohesive monolayers from mercurated calix[6]arenes. *J. Am. Chem. Soc.* **1988**, *110*, 7545–7546.

22 Markowitz, M. A.; Janout, V.; Castner, D. G.; Regen, S. L. Perforated monolayers: Design and synthesis of porous and cohesive monolayers derived from mercurated calixarenes. *J. Am. Chem. Soc.* **1989**, *111*, 8192–8200.

23 Conner, M.; Janout, V.; Regen, S. L. Molecular sieving by a perforated Langmuir−Blodgett film. *J. Am. Chem. Soc.* **1993**, *115*, 1178–1180.

24 Conner, M. D.; Janout, V.; Kudelka, I.; Dedek, P.; Zhu, J.; Regen, S. L. Perforated monolayers: Fabrication of calix[6]arene-based composite membranes that function as molecular sieves. *Langmuir* **1993**, *9*, 2389–2397.

25 Hendel, R. A.; Nomura, E.; Janout, V.; Regen, S. L. Assembly and disassembly of Langmuir−Blodgett films on poly[1-(trimethylsilyl)-1-propyne]: the uniqueness of calix-[6]arene multilayers as permeation selective membranes. *J. Am. Chem. Soc.* **1997**, *119*, 6909–6918.

26 Hendel, R. A.; Zhang, L.-H.; Janout, V.; Conner, M. D.; Hsu, J. T.; Regen, S. L. Insight into the permeation selectivity of calix[6]arene-based Langmuir−Blodgett film: Importance of head group association and the solid phase. *Langmuir* **1998**, *14*, 6545–6549.

27 Yan, X.; Janout, V.; Hsu, J. T.; Regen, S. L. The gluing of a Langmuir−Blodgett bilayer. *J. Am. Chem. Soc.* **2003**, *125*, 8094–8095.

28 Wang, M.; Janout, V.; Regen, S. L. Glued Langmuir−Blodgett bilayers from calix[n]arenes: Influence of calix[n]arene size on ionic crosslinking, film thickness, and permeation selectivity. *Langmuir* **2010**, *26*, 12988–12993.

29 Li, J.; Janout, V.; Regen, S. L. Glued Langmuir−Blodgett films: An unexpected dependency of gluing on polyelectrolyte concentration. *Langmuir* **2004**, *20*, 2048–2049.

30 Fujiwara, M.; Grubbs, R. H.; Baldeschwieller, J. D. Characterization of pH-dependent poly(acrylic acid) complexation with phospholipid vesicles. *J. Colloid Interface Sci.* **1997**, *185*, 210–216.

31 Li, J.; Janout, V.; McCullough, D. H., III; Hsu, J. T.; Troung, Q.; Wilusz, E.; Regen, S. L. Exceptional gas permeation selectivity of a glued Langmuir−Blodgett bilayer by pH control. *Langmuir* **2004**, *20*, 8214–8219.

32 Wang, M.; Janout, V.; Regen, S. L. Hyper-thin organic membranes with exceptional H_2/CO_2 permeation selectivity: Importance of ionic crosslinking and self-healing. *Chem. Commun.* **2011**, *47*, 2387–2389.

33 Robeson, L. M. The upper bound revisited. *J. Membr. Sci.* **2008**, *320*, 390–400.

34 Li, Y.; Liang, F.; Bux, H.; Yang, W.; Caro, J. Zeolite imidazolate framework ZIF-7 based molecular sieve membrane for hydrogen separation. *J. Membr. Sci.* **2010**, *354*, 48–54.

35 Yan, X.; Hsu, J. T.; Regen, S. L. Selective dampening of gas permeability of a Langmuir−Blodgett film using moist permeants. *J. Am. Chem. Soc.* **2000**, *122*, 11944–11947.

36 Wang, Y.; Stedronsky, E.; Regen, S. L. Probing the gas permeability of an ionically cross-linked Langmuir−Blodgett bilayer with a touch of salt. *Langmuir* **2006**, *24*, 6279–6284.

37 Iler, R. K. Multilayers of colloidal particles. *J. Colloid Interface Sci.* **1966**, *21*, 569–594.

38 Decher, G.; Hong, J.-D. Buildup of ultrathin multilayer films by a self-assembly process: I. Consecutive adsorption of anionic and cationic bipolar amphiphiles. *Macromol Chem., Macromol. Symp.* **1991**, *46*, 321–327.

39 Schanze, K. S.; Shelton, A. H. Functional polyelectrolytes. *Langmuir* **2009**, *25*, 13698–13702.

40 Schlenoff, J. B. Retrospective on the future of polyelectrolyte multilayers. *Langmuir* **2009**, *25*, 14007–14010.

41 Levasalmi, J.-M.; McCarthy, T. J. Poly(4-methyl-1-pentene)-supported polyelectrolyte multilayer films: preparation and gas permeability. *Macromolecules* **1997**, *30*, 1752–b1757.

42 Bruening, M. L.; Dotzauer, D. M.; Jain, P.; Ouyang, L.; Baker, G. L. Creation of functional membranes using polyelectrolyte multilayers and polymer brushes. *Langmuir* **2008**, *24*, 7663–7673.

43 Wang, Y.; Stedronsky, E.; Regen, S. L. Defects in a polyelectrolyte multilayer: The inside story. *J. Am. Chem. Soc.* **2008**, *130*, 16510–16511.

44 Li, J.; Janout, V.; Regen, S. L. Gluing Langmuir—Blodgett monolayers onto hydrocarbon surfaces. *J. Am. Chem. Soc.* **2006**, *128*, 682–683.

45 Lin, H.; Van Wagner, E.; Freeman, B. D.; Toy, L. G.; Gupta, R. P. Plasticization-enhanced hydrogen purification using polymeric membranes. *Science* **2006**, *311*, 639–642.

46 Barillas, M. K.; Enick, R. M.; O'Brien, M.; Perry, R.; Luebke, D. R.; Morreale, B. D. The CO_2 permeability and mixed gas CO_2/H_2 selectivity of membranes composed of CO_2-philic polymers. *J. Membr. Sci.* **2011**, *372*, 29–39.

47 Wang, Y.; Janout, V.; Regen, S. L. Creating poly(ethylene oxide)-based polyelectrolytes for thin film construction using an ionic linker strategy. *Chem. Mater.* **2010**, *22*, 1285–1287.